G3139, an Anti-Bcl-2 Antisense Oligomer That Binds Heparin-Binding Growth Factors and Collagen I, Alters *In vitro* Endothelial Cell Growth and Tubular Morphogenesis

C.A. Stein,[1] SiJian Wu,[1] Anatoliy M. Voskresenskiy,[1] Jin-Feng Zhou,[1] Joongho Shin,[1] Paul Miller,[2] Naira Souleimanian,[1] and Luba Benimetskaya[1]

Abstract

Purpose: We examined the effects of G3139 on the interaction of heparin-binding proteins [e.g., fibroblast growth factor 2 (FGF2) and collagen I] with endothelial cells. G3139 is an 18-mer phosphorothioate oligonucleotide targeted to the initiation codon region of the Bcl-2 mRNA. A randomized, prospective global phase III trial in advanced melanoma (GM301) has evaluated G3139 in combination with dacarbazine. However, the mechanism of action of G3139 is incompletely understood because it is unlikely that Bcl-2 silencing is the sole mechanism for chemosensitization in melanoma cells.

Experimental Design: The ability of G3139 to interact with and protect heparin-binding proteins was quantitated. The effects of G3139 on the binding of FGF2 to high-affinity cell surface receptors and the induction of cellular mitogenesis and tubular morphogenesis in HMEC-1 and human umbilical vascular endothelial cells were determined.

Results: G3139 binds with picomolar affinity to collagen I. By replacing heparin, the drug can potentiate the binding of FGF2 to FGFR1 IIIc, and it protects FGF from oxidation and proteolysis. G3139 can increase endothelial cell mitogenesis and tubular morphogenesis of HMEC-1 cells in three-dimensional collagen gels, increases the mitogenesis of human umbilical vascular endothelial cells similarly, and induces vessel sprouts in the rat aortic ring model.

Conclusions: G3139 dramatically affects the behavior of endothelial cells. There may be a correlation between this observation and the treatment interaction with lactate dehydrogenase observed clinically.

G3139 (Genasense) is an 18-mer phosphorothioate (PS) oligonucleotide that is targeted to the initiation codon region of the Bcl-2 mRNA (1). Lipid-mediated transfection of G3139 into a wide variety of tumor cells grown on plastic tissue culture plates can silence Bcl-2 mRNA and protein expression. This has been ostensibly associated with increased sensitivity to a wide variety of chemotherapeutic agents (2).

Recently, a phase III global, multicenter, randomized trial of DTIC with or without G3139 (GM301) was reported; 771 patients were randomized (3). Strikingly, a strong relationship was found between pretreatment plasma lactate dehydrogenase (LDH) and overall survival after G3139 treatment.[3] G3139 plus DTIC is clearly an active combination (versus DTIC alone) in patients with baseline LDH $\leq 1.1 \times$ upper limit of normal (508 of 771 patients randomized; $P = 0.018$ for overall survival). The survival difference is even more pronounced for patients with baseline LDH $\leq 0.8 \times$ upper limit of normal (274 of 771 patients randomized; $P = 9 \times 10^{-4}$; hazard ratio, 0.64).

Nevertheless, the mechanism of action of G3139 is not completely clear. It seems unlikely that down-regulation of the basal expression of Bcl-2 is the sole mechanism responsible for extensive chemosensitization in melanoma cells. This is especially true in light of recent results showing that multiple signaling pathways must be targeted to overcome drug resistance in cell lines derived from melanoma metastases (4).

Treatment of melanoma cells in tissue culture by lipid-transfected G3139 causes Bcl-2–independent apoptosis via the intrinsic pathway (5), characterized by lack of synergy with such cytotoxic chemotherapeutic agents as cisplatin, Taxotere, and thapsigargin (6). Bcl-2 silencing by RNAi in melanoma cells also did not produce synergy with cytotoxic chemotherapy (6), although in other laboratories *in vitro* synergy with chemotherapy in melanoma cells has been reported (7). The combination of G3139 plus cytotoxic chemotherapy treatment can indeed produce responses in human melanoma xenografts

Authors' Affiliations: [1]Department of Oncology, Albert Einstein-Montefiore Cancer Center, Montefiore Medical Center, Bronx, New York and [2]School of Public Health, Johns Hopkins University, Baltimore, Maryland

Received 10/8/08; revised 1/6/09; accepted 1/8/09; published OnlineFirst 4/7/09.

Grant support: NIH grant CA108415 (C.A. Stein).

The costs of publication of this article were defrayed in part by the payment of page charges. This article must therefore be hereby marked *advertisement* in accordance with 18 U.S.C. Section 1734 solely to indicate this fact.

Note: Supplementary data for this article are available at Clinical Cancer Research Online (http://clincancerres.aacrjournals.org/).

Requests for reprints: C.A. Stein, Montefiore Medical Center, Albert Einstein College of Medicine, 111 East 210 Street, Bronx, NY 10467. Phone: 718-920-8980; Fax: 718-652-4027; E-mail: cstein@montefiore.org.

doi:10.1158/1078-0432.CCR-08-2610

[3] S. Agarwala, et al., submitted for publication.

Translational Relevance

A randomized, global phase III trial of G3139 in combination with dacarbazine versus dacarbazine alone was completed in patients with advanced melanoma, and a confirmatory trial of G3139 plus dacarbazine is currently under way in patients with advanced melanoma and low to normal baseline lactate dehydrogenase. G3139 was designed to target and silence the Bcl-2 mRNA, producing, in theory, chemosensitization. It seems, however, that this may, in fact, be one of the several mechanisms that contribute to the effectiveness of the drug. Given the clinical interest in G3139, it is thus of critical importance to the continued development of oligonucleotide therapeutics for cancer to further elucidate the basis of this activity.

in severe combined immunodeficient mice (8). However, experiments with PS oligomers in severe combined immunodeficient mice are difficult to interpret with respect to determination of mechanism (8). This is because of the Toll-like receptor-9 active properties of virtually all PS oligomers (9), even those that do not contain CpG motifs; G3139 contains two such motifs. Thus, tumor inhibition due to immunostimulation (leading to increased levels of tumoricidal IFN-α and interleukin-12) cannot readily be distinguished from tumor inhibition due to gene silencing.

In vivo, the endothelial cell is exposed to steady-state plasma levels of oligonucleotide (for up to 5 days in the GM301 trial) that may approach 1 μmol/L (10). This cell type is critical to the growth and metastasis of tumors and in tumors exposed to the highest levels of oligonucleotide (11). However, the effects of G3139 on this cell type have not, to our knowledge, been elucidated. Whereas it is known (12) that compounds closely related to G3139 can bind fibroblast growth factor 2 (FGF2), the consequences of such binding have never been explored appropriately. Herein, we present evidence that G3139 may nonspecifically bind to several heparin-binding proteins (e.g., FGF2, collagen I) that dramatically affect endothelial cell function. We also show that G3139 can increase endothelial cell mitogenesis and tubular morphogenesis in three-dimensional collagen gels and can induce vessel sprout formation in the aortic ring assay.

Materials and Methods

Cells. SV40-transformed HMEC (HMEC-1) cells were obtained from the Centers for Disease Control and grown in MCDB 131 medium supplemented with 10% heat inactivated fetal bovine serum, 10 ng/mL epidermal growth factor, 1 μg/mL hydrocortisone, 100 units/mL penicillin G sodium, and 100 μg/mL streptomycin sulfate. The stock culture was maintained at 37°C in a humidified 5% CO_2 incubator. BaF3 cells transfected with FGFR1 IIIc (C11 clone) were a kind gift of Dr. D.M. Ornitz (Washington University, St. Louis, MO) and were grown in RPMI 1640 + 10% newborn bovine serum, 0.5 ng/mL murine recombinant interleukin-3, 2 mmol/L L-glutamine, penicillin-streptomycin, 50 nmol/L β-mercaptoethanol, and G418 (600 mg/mL). The stock cultures were maintained at 37°C in a humidified 5% CO_2 incubator.

Materials. Recombinant human FGF2, vascular endothelial growth factor (VEGF)-165, platelet-derived growth factor-BB (PDGF-BB), and heparin-binding epidermal growth factor were from R&D Systems. MCDB 131 and fetal bovine serum were obtained from Invitrogen. ^{125}I-FGF2 and ^{125}I-VEGF were purchased from Perkin-Elmer. The IMUBIND Total TFPI ELISA kit was from American Diagnostica. The human FGF2 ELISA kit was purchased from R&D Systems. Collagen I was from BD Biosciences. Rhodamine phalloidin was from Invitrogen-Molecular Probes.

Modification of heparin-binding proteins by ClRNH^{32}P-OdT$_{18}$. The probe, radiolabeled, alkylating oligodeoxynucleotide ClRNH^{32}P-OdT$_{18}$, was synthesized as per Guvakova et al. (12). Determination of the Michaelis constant (K_M) for the binding of the probe for PDGF-BB, VEGF165, and collagen I was by the method of Yakubov et al. (13). For K_c determination, FGF2 (50 nmol/L), PDGF-BB (50 nmol/L), VEGF165 (150 nmol/L), or collagen I (30 nmol/L) was incubated in 0.1 mol/L Tris-HCl (pH 7.4), containing 10 to 20 μmol/L ClRNH^{32}P-OdT$_{18}$. PS oligo was added at increasing concentrations as competitors of the binding of the probe oligomer. After 1 h at 37°C, SDS-PAGE was done, and the gel allowed to expose Kodak X-ray film until bands were visualized. These were quantitated by laser densitometry; the IC_{50} of competition was determined; and K_c was calculated by the Cheng-Prusoff (14) relationship $K_c = IC_{50} / (1 + [ClRNH^{32}P\text{-}OdT_{18}] / K_d)$.

Displacement of extracellular matrix–bound ^{125}I-FGF2 by G3139. Bovine eyes were obtained from Morris Insel Cohen, and extracellular matrix (ECM) was prepared by previous methods (15). Dextran T-40 (5%) was included in the growth medium and the cells were incubated for 10 to 12 d at 37°C in 10% CO_2. After NH_4OH treatment to remove the corneal cells, the ECM was stored at 4°C.

For release experiments, ECM was incubated (3 h, room temperature) with ^{125}I-FGF2 (2.5×10^4 cpm/0.3 mL/well) in PBS + 0.02% gelatin. Unbound radiolabeled protein was removed by washing thrice with PBS + 0.02% gelatin, and the ECM was incubated with increasing concentrations of PS oligo at room temperature for 3 h. The amount of released ^{125}I-FGF2 was determined by gamma-counting. The remaining ECM was incubated (3 h, 37°C) with 1 N NaOH and counted. The percentage of released ^{125}I-FGF2 was calculated from the total ECM-associated radioactivity. For all experiments, measurements were made in duplicate (each duplicate was repeated thrice) with average differences no greater than 5% between the replicates.

Protection of FGF2 by PS oligos against protease digestion. FGF2 or VEGF165 (~0.5 μg in total volume 20 μL, pH 7.4) with tracer amounts of ^{125}I-FGF2 or ^{125}I-VEGF165 in the presence or absence of G3139 (5 μmol/L) was equilibrated at 37°C for 5 min. Trypsin or chymotrypsin was added to a final concentration of 1 μg protease/50 μg FGF2 or VEGF165, and digestion was allowed to proceed at 37°C for 4 h. SDS gel sample buffer was then added; the samples were heated at 100°C for 5 min; and SDS-PAGE was done. The gels were dried and allowed to expose Kodak X-ray film until bands were visualized, which were quantitated by laser densitometry. To air oxidize FGF2, 20 ng/mL in complete medium were incubated at 37°C in room air for 3 h. Under these conditions, as described in Results, all FGF2 activity is lost.

FGF2-induced mitogenesis in C11 cells. C11 (FGFR1 IIIc–overexpressing) cells were washed twice with RPMI medium lacking interleukin-3 and plated at 2.2×10^4 per well in 48-well plates. FGF2 (1 nmol/L), PS oligo, or heparin (1 μg/mL) was added in a total volume 200 μL. The cells were then incubated for 2 to 3 d, fixed, and stained with sulforhodamine blue. The absorbance at $\lambda = 530$ nm was taken as proportional to cell number.

Three-dimensional collagen I gels. Collagen I gels were formed by mixing M199 medium containing 10% fetal bovine serum + penicillin/streptomycin (basal medium), 1 N NaOH (0.023 × volume of collagen I), and collagen I at a final concentration of 0.6 mg/mL (4°C). Aliquots of the mixture (0.25 mL) were dispensed into 24-well plates and allowed to gel at 37°C for 2 h. HMEC-1 cells were seeded onto the collagen I gels (10×10^4 per well) in basal medium. Three hours later, the attached cells were overlaid with a second layer of collagen I, and

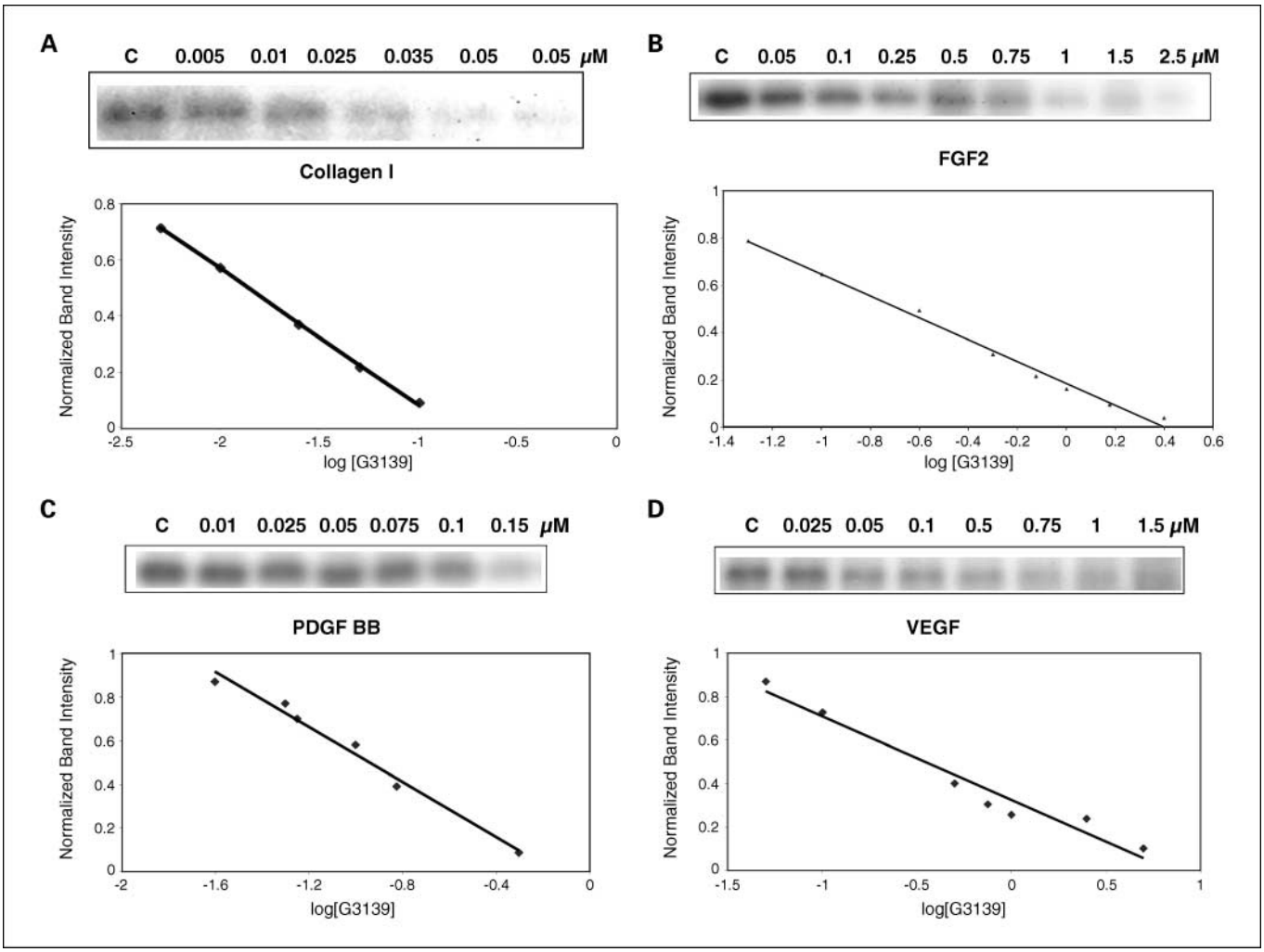

Fig. 1. Competition by G3139 for binding of $ClRNH^{32}P\text{-}OdT_{18}$ to collagen I (*A*), FGF2 (*B*), PDGF BB (*C*), and VEGF (*D*). G3139 was used as a competitor at the stated concentrations for the binding of the probe ($ClRNH^{32}P\text{-}OdT_{18}$) to the respective heparin-binding proteins, as described in Materials and Methods (*left*; 12% PAGE). After determination of the IC_{50} of competition from the plot of normalized band intensity versus log [G3139] (*right*), values of K_c were determined by the Cheng-Prusoff equation.

0.5 mL basal medium ± PS was added above the second layer. PS oligomer was added every 3 d.

After 6 d, cells were fixed with 4% paraformaldehyde + 0.25% glutaraldehyde in PBS at room temperature overnight and permeabilized with 0.2% Triton X-100 for 30 min. After washing, the cells were stained with rhodamine phalloidin (160 nmol/L). Tubular morphogenesis was monitored by confocal microscopy and quantitated by ImageJ software (n = 3). To liberate cells, the three-dimensional collagen gels were treated with 0.1% collagenase type I in PBS for 30 to 40 min at 37°C, washed with PBS, and centrifuged. Cells were counted by trypan blue exclusion (n = 3).

Radial invasion of matrix by aggregated cells. A modification of the method of Vernon and Sage (16) was used. Dispersed HMEC-1 cells (180×10^4/mL in basal medium) were cultured in 40-μL drops suspended upside down from 12-well plate lids lined with Parafilm M. After 2 d in culture, aggregates of cohesive cells (one aggregate per drop) were transferred into wells (12-well plates), which had been prefilled with 0.5 mL of a 0.6 mg/mL collagen type I gel. Aggregate transfer was accomplished by depressing, and therefore stretching, the parafilm until the drops containing the cells touched the polymerized collagen I. The cell aggregates were then overlaid with a second layer of collagen gel, and 1 mL basal medium with or without either FGF2 (20 ng/mL) or PS oligo (1 μmol/L), or a combination of both, was added above the second layer. The cells were cultured for 2 to 5 d at 37°C in a humidified 5% CO_2 incubator and photographed daily. The average distances of migration of the HMEC cells into the surrounding collagen, calculated from 9 to 12 replicates, were averaged to yield the final values of radial invasion.

Confocal microscopy. Images were collected with a Bio-Rad Radiance 2000 laser scanning confocal microscope (Zeiss) with a Kr/Ar laser for excitation at 568 nm, narrow band filters for emission, and a Nikon 20× PlanApo optics on an Eclipse 200 laser-safe microscope. Images were analyzed by the use of ImageJ software.[4]

Rat aortic ring assay. Following established procedures (17), thoracic aortas were obtained from CO_2-sacrificed 1- to 2-mo-old Fisher 344 male rats. Aortas were sectioned into 1-mm rings, rinsed in 12 consecutive washes of serum-free medium, and the rings embedded in 0.6 mL of collagen type I gel (1 mg/mL) in M131 complete medium + 10% fetal bovine serum. One hour later, the cultures with the embedded aortas (n = 6) were treated with 1 μmol/L G3139, and the media changed, with new G3139 added, every other day. Phase-contrast photomicrographs were taken daily after treatment. The numbers of vessels were counted, and their lengths (the five longest vessels in

[4] http://rsb.info.nih.gov/ij/

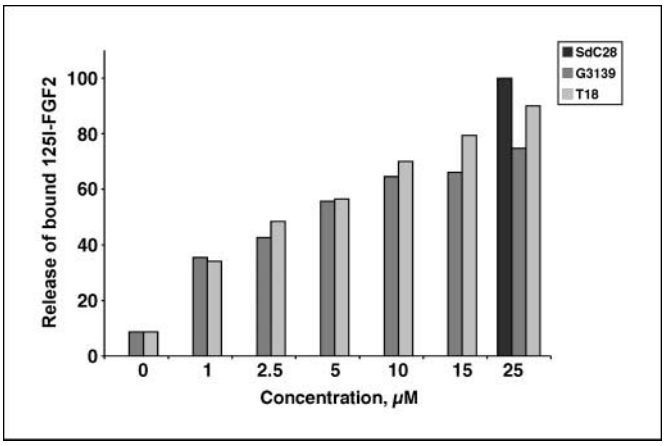

Fig. 2. Release of ECM-bound ^{125}I-FGF2 by G3139 and T_{18}. ECM-coated wells were incubated (3 h, room temperature) with ^{125}I-FGF2 (2.5×10^4 cpm/well). The ECM was washed thrice and incubated (3 h, room temperature) with increasing concentrations of G3139 or T_{18}. Released radioactivity is expressed as the percent of total ECM-bound ^{125}I-FGF2 and is compared with release by 25 μmol/L SdC28. Each assay was conducted in duplicate and the differences in the duplicate measurements were <10%. Experiments were repeated thrice.

five rings) measured (17) visually with a micrometer scale in the microscope eyepiece. Data are expressed as the average vessel number or length ± SD. *P* values were calculated by the Mann-Whitney test.

Statistics. Unless otherwise mentioned, experiments were done at least in triplicate, and data are presented as the average ± SD. *P* values were determined by a two-sided Student's *t* test with unequal variance, with $P < 0.05$ considered significant.

Results

PS oligos interact with heparin-binding proteins. We used the Cheng-Prusoff relationship to determine the K_c (competition constant) of binding of G3139 and other PS oligos to several heparin-binding proteins; these included including FGF2, VEGF165, PDGF-BB, and collagen I. The determination of K_c initially required the measurement of K_M of binding to each test protein of a probe oligonucleotide. This probe is an alkylating, ^{32}P-labeled phosphodiester 18-mer homopolymer of thymidine (ClRNH^{32}P-OdT_{18}). For FGF2, K_M = 0.5 μmol/L (12). As previously shown (18) for the other proteins above, the binding of the probe was approximately saturable and was described by a single-site binding equation of the Michaelis-Menton type. $-1/K_M$ was then determined by double-reciprocal Lineweaver-Burke plots. By least squares analysis, these plots for each protein were linear. The values of K_M for VEGF165, PDGF-BB, and collagen I were 34, 4.5, and 0.6 μmol/L, respectively.

In Fig. 1, competition for probe binding to collagen I (Fig. 1A), FGF2 (Fig. 1B), PDGF-BB (Fig. 1C), and VEGF165 (Fig. 1D) is shown. The IC_{50}s of competition were determined, and the values of K_c for each protein and the values of K_c were 50 nmol/L and 1.2 μmol/L for PDGF-BB and VEGF165, respectively. The K_c of binding of G3139 to FGF2 based on our previous experiments (12) is ~50 nmol/L.

Due to its high lysine content, collagen I is a basic protein. Collagen I, in monomeric form, bound with high affinity to the probe oligonucleotide (K_M = 0.6 μmol/L; R^2 = 0.95). When G3139 was used as a competitor of probe binding, K_c = 400 pmol/L (R^2 = 0.99). This, we believe, is the highest affinity interaction for any nonspecific oligonucleotide-protein binding yet determined and is probably indicative of strong electrostatic interactions between polyanionic PS oligonucleotides and basic collagen I.

The K_c of G3139 competition for the binding of the probe to VEGF165 (K_c = 285 nmol/L, R^2 = 0.92; Fig. 1D) is, in contrast, much greater than that of both collagen I and FGF2. Relatively low-affinity interactions were also observed between laminin and G3139 (K_c = 115 nmol/L; R^2 = 0.97; data not shown). Heparin-binding epidermal growth factor also interacted with G3139 (K_c = 20 nmol/L, R^2 = 0.99).

G3139 releases ^{125}I-FGF2 from low-affinity binding sites on ECM. ECM contains numerous low-affinity sites (K_d = 1-10 nmol/L) that interact with FGF2 (19). The protein can be readily isolated from polyanion-treated matrix (20), and mobilization of matrix-bound FGF2 is thought to promote endothelial proliferation (21).

We adsorbed ^{125}I-FGF2 to bovine corneal endothelial matrix–coated dishes, which were then treated with G3139. The maximal release of ^{125}I-FGF2 was compared with release by SdC28, a 28-mer PS homopolymer of cytidine: This was arbitrarily assigned a value of 1. The release of ^{125}I-FGF2 bound to the ECM by SdC28 and 2 mol/L NaCl were identical. As shown in Fig. 2, release was G3139 concentration dependent. However, there was little or no release of ECM-bound ^{125}I-VEGF165 by G3139 at any concentration evaluated (up to 100 μmol/L; data not shown). These data are consistent with our previous experiments showing the low affinity of G3139 for VEGF165.

G3139 potentiates the binding of FGF2 to FGFR1 IIIc (C11 clone). It was our hypothesis that G3139 could substitute for heparin and thus increase the mitogenic effects of FGF2 on endothelial cells. FGF2 binds with high affinity to FGFR1 (22); BAF3 cells transfected with FGFR1 IIIc require heparin or heparin-like activity (which on occasion can be found in serum) to proliferate in response to FGF2 (23). As determined by sulforhodamine blue staining, cellular mitogenesis was

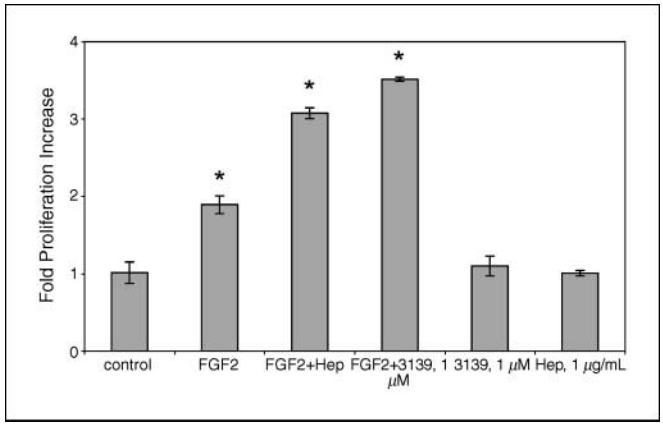

Fig. 3. G3139 substitutes for heparin, which is required for the biological activity of FGF2. C11 cells were washed twice with medium without interleukin-3 and seeded (2.2×10^4 per well in 48-well plates) in medium containing 10% fetal bovine serum but not interleukin-3. The cells were then treated with 1 nmol/L FGF2 + G3139 (1 μmol/L). After 2 d, proliferation was evaluated by sulforhodamine blue staining. Columns, average (n = 3); bars, SD. FGF2 + Hep versus FGF2: $P < 0.001$; FGF2 + G3139 versus FGF2: $P < 0.002$; G3139 or Hep versus control: $P > 0.05$ (not significant). Hep, heparin.

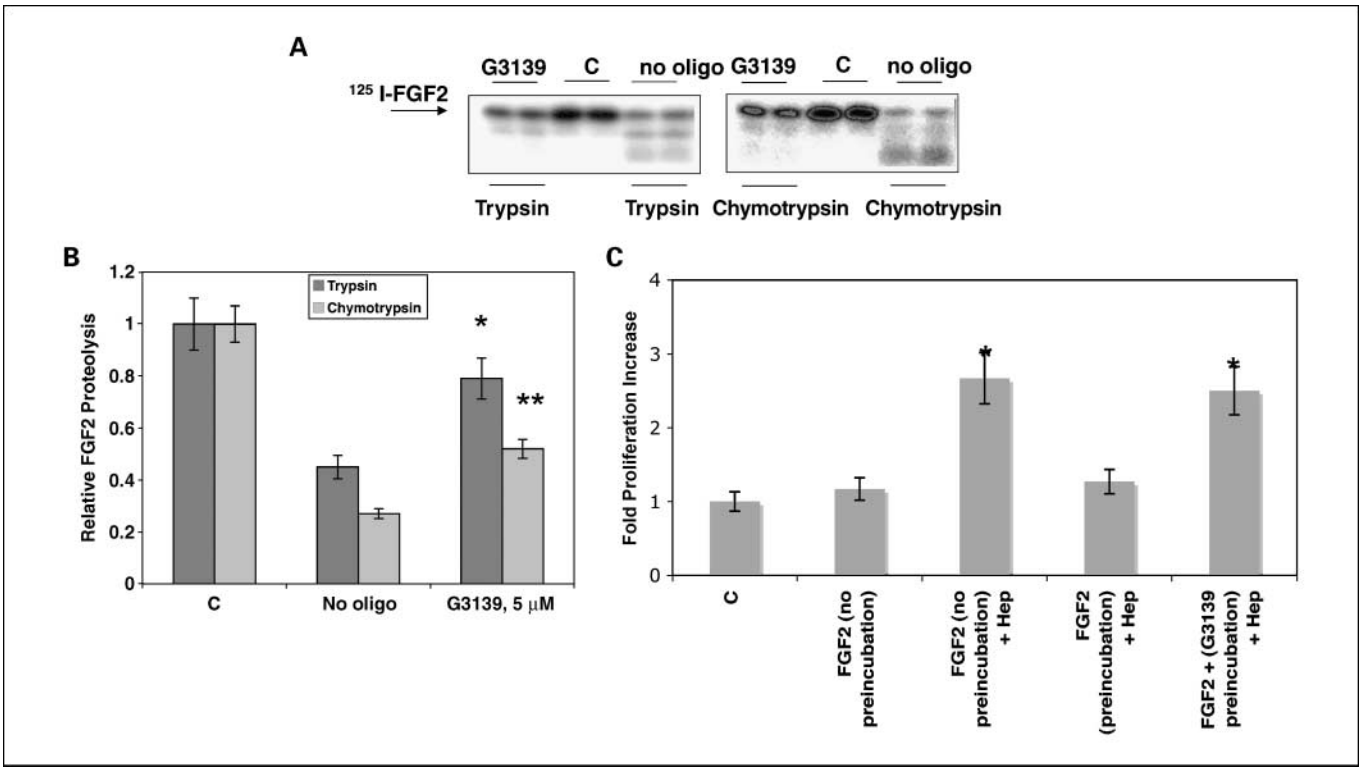

Fig. 4. Preincubation with G3139 protects FGF2 from degradation by trypsin and chymotrypsin. FGF2 (*A* and *B*; ~0.5 μg in 20 μL, pH 7.4) containing tracer amounts of [^{125}I]-FGF2 was digested with either 2% trypsin or chymotrypsin (w/w) in the absence or presence of 5 μmol/L G3139 (37°C, 4 h). The digestion products were mixed with sample buffer, boiled for 5 min, and analyzed by 12% SDS-PAGE. Gel bands were quantitated by laser densitometry. Columns, average (n = 3); bars, SD. *, $P < 0.05$; **, $P < 0.03$, versus no oligo. C, no trypsin, no G3139. *C,* G3139 protects FGF2 from inactivation at 37°C. FGF2 was incubated at 37°C for 3.5 h with or without 5 μmol/L G3139 and added to the C11 FGFR1 IIIc – overexpressing cells (2.2×10^4 cells per well in 48-well plates) in the presence of heparin. Cell proliferation was measured after 3 d by sulforhodamine blue. FGF2 (1 nmol/L) without preincubation at 37°C for 3.5 h was used as a positive control. Columns, average (n = 3); bars, SD. *, $P < 0.03$, versus FGF2 + preincubation at 37°C for 3.5 h.

evaluated in the presence of 1 nmol/L FGF2 and G3139 (1 μmol/L). Proliferation of the transfectants was increased by 3.5 ± 0.03-fold compared with the non–G3139/FGF2-treated cells (n = 3; P = 0.002) and was approximately twice that observed after FGF2 treatment alone (Fig. 3). No increase in proliferation was produced by heparin (1 μg/mL) or G3139 (1 μmol/L) alone. Treatment of HMEC-1 cells cultured on plastic with 10 to 50 ng/mL FGF2 increased proliferation by ~40% to 50% after 6 days. However, the FGF2-induced increase in HMEC-1 cell proliferation was not changed by G3139.

These experiments definitively show that G3139 can substitute for heparin in promoting the proliferation of FGF2-dependent cells. In addition, they also prove that G3139, despite its interactions with low-affinity binding sites on FGF2, does not interfere with the binding of this protein to high-affinity (K_d = 2×10^{-11}-20×10^{-11} mol/L; ref. 24) cell surface receptors.

G3139 protects FGF2 from enzymatic digestion and air oxidation. In the interior of a poorly vascularized tumor, cellular necrosis can occur, and necrotic cells can release proteases. Therefore, we wanted to determine the extent to which the binding of G3139 to FGF2 could protect it against proteolytic degradation. Two potent proteases were used (Fig. 4A and B). ^{125}I-FGF2 was degraded by trypsin (37°C, 2 hours, pH 7.4) but was partially protected from cleavage by the protease in the presence of G3139 or other PS oligomers, including L-G3139 (1 μmol/L; data not shown), which is the L-enantiomer of D-G3139. FGF2-G3139 complexes were also exposed to chymotrypsin (37°C, 2 hours). In the absence of G3139, FGF2 was degraded by chymotrypsin. In the presence of G3139, FGF2 was partially protected from degradation. We also investigated the degradation of VEGF165-G3139 complexes by trypsin and showed that there was no protection (data not shown). This experiment is consistent with the low affinity of VEGF165 for G3139 relative to FGF2.

In addition, after exposure to air at 37°C, FGF is inactivated relatively rapidly, probably due to oxidation at cysteine thiol, as has been shown for FGF1 (25). We incubated FGF2 in complete medium at 37°C for 3.5 h with or without 5 μmol/L G3139, and then used this mixture, in the presence of heparin, to treat the FGFR1-transfected BAF3 cells. If FGF2 was not preincubated with G3139, it was presumably susceptible to air oxidation; in this case, there was no increase in the proliferation of the FGFR1 IIIc transfectants in the presence of heparin versus control cells not treated with FGF2. However, if we used FGF2 that had been pretreated with G3139, FGF2-dependent proliferation increased 3-fold versus control (Fig. 4C) to an essentially normal level.

G3139 stimulates tubular morphogenesis and mitogenesis of HMEC-1 cells in three-dimensional collagen I gels. Only minimal morphologic effects or changes in cell proliferation were produced after treatment of HMEC-1 cells on plastic plates or in two-dimensional collagen I or collagen IV gels (up to

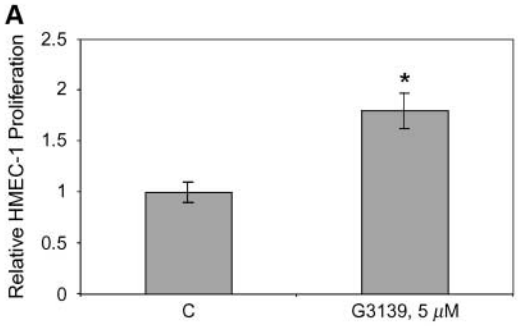

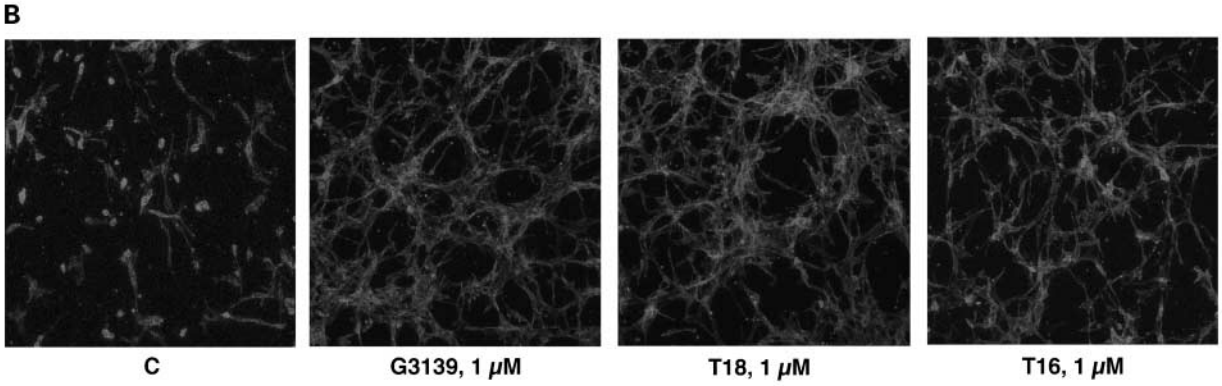

Fig. 5. *A,* G3139 increases HMEC-1 proliferation in three-dimensional collagen I gels. Cells (45×10^4 per well in six-well plates) were seeded in three-dimensional collagen I gels (0.6 mg/mL) and treated with G3139 (5 μmol/L). Cells were counted on day 6. Columns, average of triplicate wells; bars, SD. Relative HMEC-1 proliferation, 1.8 ± 0.18-fold, $n = 3$ [$P < 10^{-2}$, G3139 (5 μmol/L) versus C (no treatment)]. *B,* confocal micrograms of HMEC-1 cells in three-dimensional collagen I gels after 6 d in culture. HMEC-1 cells (10×10^4 per well) were seeded in collagen I (0.6 mg/mL) and treated with G3139, T_{18}, or T_{16} (1 μmol/L) or were untreated (*C*). At the end of treatment (6 d), the cells were fixed permeabilized and stained with rhodamine phalloidin (160 nmol/L).

40 μmol/L G3139, 6 days). However, in three-dimensional collagen I gels + complete medium, the number of HMEC-1 cells, after treatment with 1 μmol/L G3139 every 3 days for 6 days, increased by 1.8 ± 0.4-fold ($n = 3$; $P < 0.015$) versus control, non–G3139-treated cells (Fig. 5A). (In the absence of collagen I, the increase in proliferation in similarly treated cells is only ~20%.) In addition, by 6 days, the G3139-treated, but not the untreated, cells underwent tubular morphogenesis (Fig. 5B). Examination of the time course of this effect showed that by 1 to 2 days, the cells extended fine, long apical branches. By 3 to 4 days, the cells lined up along these branches; at about the same time, cell body fusion could be observed. By 6 to 9 days, cells became organized into tube-like structures. After 9 to 11 days, the tubes began to dissolve. However, the effect is not sequence specific because T_{18} is as active as G3139, but it is length dependent because T_{16} is less active than T_{18}.

Quantitation of the extent of tubular structure formation in the rhodamine phalloidin–stained cells, after fixation, was accomplished by confocal microscopy and ImageJ software. A "streak" pattern was obtained via the initial analysis: This pattern was skeletonized (Fig. 5B) and subsequently quantitated (Fig. 6A). The tubular morphogenesis of HMEC-1 cells in three-dimensional collagen I gels was increased ~8-fold by either G3139 or T_{18} (1 μmol/L) after skeletonization versus the non–G3139-treated control cells (Fig. 6B). The effects of G3139 are highly concentration dependent (Figs. 7 and 8A-B) and are lost at [G3139] = 0.25 μmol/L.

G3139-protected FGF2 promotes HMEC-1 mitogenesis in three-dimensional collagen I gels but does not promote radial cellular outgrowth. The ability of FGF2 to induce the mitogenesis of FGFR1 IIIc–transfected BAF-3 cells (C11 cells) was completely lost when the protein was incubated in air at 37°C for 3.5 hours, as described above. When HMEC-1 cells in three-dimensional collagen I gels were incubated with air-oxidized FGF2 (20 ng/mL), mitogenesis was similarly blocked. In contrast, FGF2-induced mitogenesis was restored to normal levels (Fig. 9A and B) when the HMEC-1 cells embedded in collagen I were treated with preincubated FGF2. Here, G3139 (5 μmol/L) had been added to the preincubation buffer only.

Nevertheless, in the induction of radial invasion of matrix (here three-dimensional collagen I gels), G3139 does not protect FGF2. In the radial invasion of matrix by aggregated cells (RIMAC) model, after 2 to 3 days, FGF2 (20 ng/mL) induced measurable HMEC-1 radial invasion (2.5-fold versus control; average, 0.75 versus 0.3 mm; $n = 6$). However, radial invasion was not induced by either G3139 alone (1 μmol/L) or FGF2 preincubated in air (37°C, 3.5 hours; Supplementary Fig. S1). We had initially hypothesized that FGF2 preincubated with 1 μmol/L G3139 would be protected in its ability to induce radial invasion of HMEC-1 cells in three-dimensional collagen I gels. However, this was not the case because we observed only a minimal to no increase in radial invasion (versus no added FGF2). Therefore, it is possible that FGF2 has two distinct functions. G3139, which binds at the heparin-binding site, protects induction of cellular mitogenesis by FGF2. G3139, however, does not protect the induction of radial migration by FGF2, perhaps implying that the molecular epitope responsible for this is possibly distant and distinct from the heparin-binding site.

G3139 promotes the growth of human umbilical vascular endothelial cells. It was exceptionally difficult to coax human umbilical vascular endothelial cells (HUVEC) to grow either on plastic or on plastic with collagen I gel (2 mg/mL)

underneath, and in three-dimensional collagen I gels, cell growth was minimal. We plated cells on plastic with collagen I gel underneath and treated them with G3139 (20 μmol/L; Supplementary Fig. S2). Cellular proliferation, as determined after collagenase digestion and counting by trypan blue exclusion (n = 4, P versus untreated for all experiments), increased by 2.2 ± 0.2-fold (2.2×10^4 versus 1.1×10^4 cells per well, $P < 10^{-4}$). This increase was only slightly less than what we observed with heparin, the standard growth additive for HUVEC cells (2.7 ± 0.2-fold, $P < 10^{-4}$). When plated on plastic alone, G3139 (20 μmol/L) increased cellular mitogenesis by only 1.7 ± 0.03-fold ($P < 10^{-7}$), compared with 2.7 ± 0.05-fold ($P < 10^{-6}$) for heparin. Qualitatively, these data are similar to what we observed in G3139-treated HMEC-1 cells. The increase in proliferation was accompanied by a dramatic increase in F-actin stress fibers, observable after rhodamine phalloidin staining, as shown in Supplementary Fig. S2.

G3139 promotes vessel sprout formation in the rat aortic ring assay. When 1-mm-thick rat aortic rings were embedded in three-dimensional collagen I gels and treated with 1 μmol/L G3139 with medium changes every other day, on average 3.5-fold more vessel sprouts emerged after 4 days from each G3139-treated ring than from control, untreated specimens [35 ± 9 versus 10 ± 6 (n = 6), $P = 5 \times 10^{-3}$; Supplementary Fig. S3]. Vessel sprouting was significantly (~50%) diminished when the G3139 concentration was increased to 5 versus 1 μmol/L, probably due to toxicity. In addition, the vessels in the 1 μmol/L G3139–treated aortas were substantially longer (41 ± 12 μm, n = 30 vessels measured) than those in the control, untreated aortas (24 ± 12 μm, n = 24; $P < 10^{-4}$).

Discussion

The complete mechanism of action of G3139, a drug been studied in advanced melanoma, is not yet known. Data presented in this study indicate that G3139 can potentiate the binding of FGF2 to its high-affinity cell surface receptors, here FGFR1 IIIc. Reexamination of seemingly contradictory early data suggesting inhibition of high-affinity receptor binding (12) actually reveals that inhibition is confined to longer PS oligomers at higher concentrations than used here and is in any case minimal.

In addition, G3139, at a physiologically attainable concentration for HMEC-1 cells (HUVEC cells require higher concentrations), dramatically increases endothelial cell mitogenesis and tubular morphogenesis in three-dimensional collagen I gels. The potential significance of this observation has been described by Liu and Senger (26). When endothelial precursor cells contact collagen I–containing matrix in the embryo, they align into solid pre-capillary cord-like structures that are interconnected to form a polygonal network. This morphogenic program can be mimicked in mature endothelial cells after degradation of basement membrane and subsequent contact with collagen I. Collagen I then drives the morphogenesis of new vessel sprouts, in part by inducing G-actin to F-actin polymerization in the endothelial cells (27), as we observed in primary HUVECs.

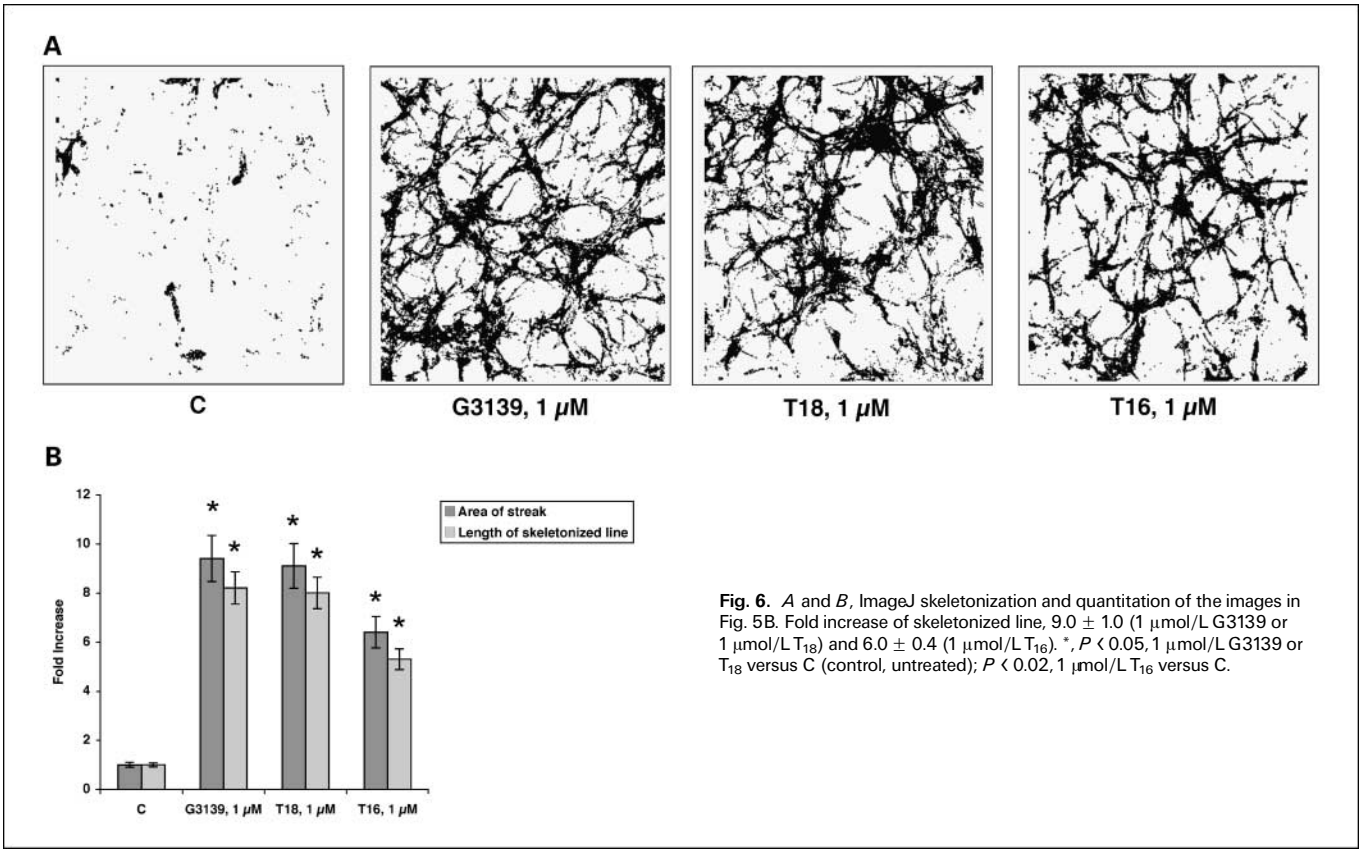

Fig. 6. *A* and *B*, ImageJ skeletonization and quantitation of the images in Fig. 5B. Fold increase of skeletonized line, 9.0 ± 1.0 (1 μmol/L G3139 or 1 μmol/L T_{18}) and 6.0 ± 0.4 (1 μmol/L T_{16}). *, $P < 0.05$, 1 μmol/L G3139 or T_{18} versus C (control, untreated); $P < 0.02$, 1 μmol/L T_{16} versus C.

The interaction of G3139 and FGF2 affects endothelial cell function. Mobilization of FGF2 from its low-affinity glycosaminoglycan binding sites on ECM increases the radius of its activity (28). FGF2 has long been known to promote microvessel formation (29) and, unlike VEGF, also produces chemoresistance in endothelial cells by promotion of a complex between Raf-1 and ASK1 (30). This complex neutralizes the proapoptotic activity of ASK1 by blocking its translocation to the mitochondrial outer membrane.

Addition of FGF2 to endothelial cells (31) or stromal cells (32) in culture can also result in the expression of the highly proangiogenic protein VEGF. However, FGF2 and VEGF have different effects on blood vessel maturation and function (33). For example, gene transcripts are differentially modified by the two growth factors (34), and increased endothelial fenestration is observed in VEGF-overexpressing, but not FGF-overexpressing, cells (35).

Thus, agents that potentiate the effects of FGF2 stimulate angiogenesis. G3139 mobilizes FGF2 from its low-affinity binding sites on ECM, potentiates FGF2 binding to FGFR1 IIIc, and protects FGF2 against proteolysis. The effects of G3139 on endothelial cells *in vitro* may be mediated by its very high affinity for collagen I, one of the most important protein inducers of angiogenesis. Taken in toto, the behavior of the 18-mer G3139 is very similar to that of defibrotide, which is also an angiogenesis-altering agent. Defibrotide is a polydisperse mixture of single-stranded phosphodiester oligonucleotides (range, 9- to 80-mer; average, 50-mer) derived from porcine intestines. As shown in several phase II clinical trials (e.g., ref. 36), defibrotide can be curative for patients with chemotherapy-induced severe hepatic veno-occlusive disease, an entity characterized by profound hepatic sinusoidal angiotoxicity, which leads to hepatic hypoxia, dysfunction, and death.

This discussion raises a question. Usually, it is antiangiogenic, not proangiogenic, strategies that are thought important in anticancer therapeutics. However, as noted by Jain (37, 38), this is the paradox of antiangiogenic therapy. If the vasculature of a tumor is destroyed, the delivery of oxygen is diminished, producing hypoxia, which would diminish the effectiveness of cytotoxic chemotherapy. This diminution may occur possibly because of induction of the hypoxia-inducible factor-1α transcription factor, which is a major hypoxia sensor (39) responsible for the up-regulation of numerous antiapoptotic (e.g., *ADM*, *IGF2*, and *TGFA*) and proinvasion and prometastasis genes (e.g., *UPAR* and *MMP2*). Hypoxia-inducible factor 1α also stimulates VEGF and VEGFR2 expression (40), which induce abnormalities (e.g., vascular leakiness) in the tumor vasculature. Interestingly, Bcl-2 overexpression in melanoma cells also seems to increase hypoxia-inducible factor 1α, and hence VEGF, activity (41).

Hypoxia can also induce genetic instability that can select for tumor cells with increased metastatic potential (42) and can, via c-met proto-oncogene activation, lead to cells that are more aggressive and invasive (43). Diminished blood flow and low pH can also compromise the functions of tumor-infiltrating immune effector cells and cytokines. Clinical studies (44) have shown that the presence of hypoxic regions within tumors correlates with poor prognosis and increased metastatic risk regardless of treatment (i.e., what is observed in advanced melanoma).

What relevance do these facts have to the clinical situation in advanced melanoma patients treated with G3139 as part of the GM301 trial? We raise the possibility that transient, local

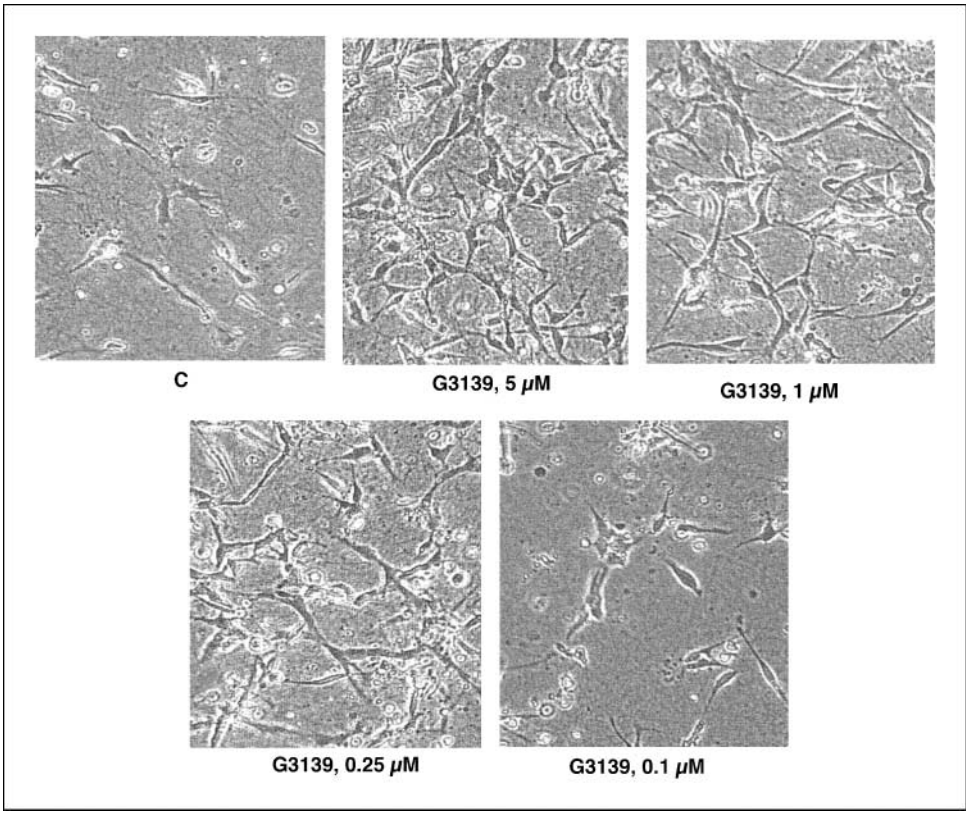

Fig. 7. Light microscopic images of the concentration dependence of HMEC-1 tubular morphogeneis in three-dimensional collagen gels as induced after 6 d by G3139.

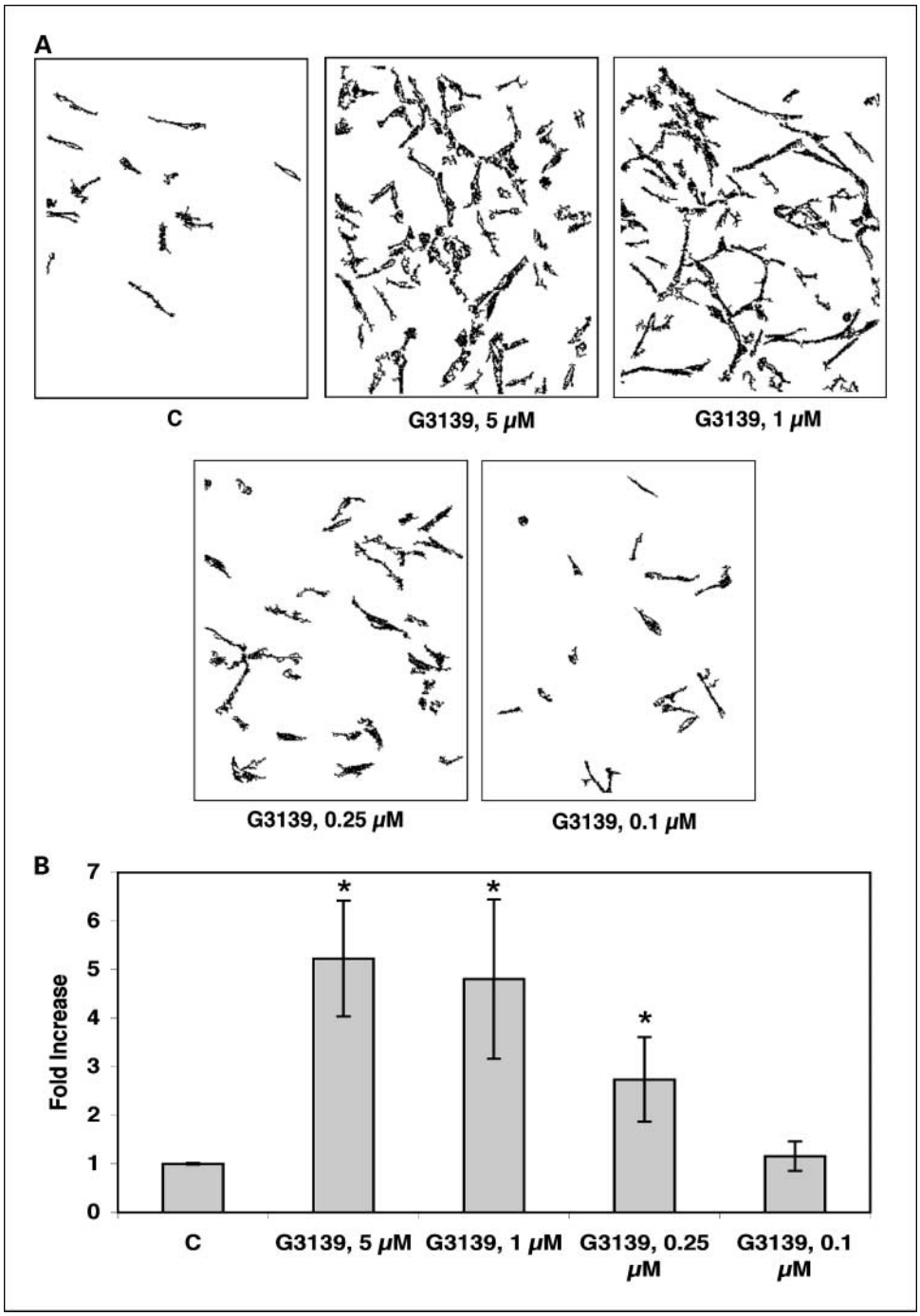

Fig. 8. *A* and *B,* quantitation of skeletonization by ImageJ of the confocal micrograms of HMEC-1 cells in three-dimensional collagen I gels in Fig. 7. Each experiment was done in triplicate. *, $P < 0.05$, G3139 at 5, 1, or 0.25 μmol/L versus C (control, untreated); 0.1 μmol/L G3139 versus C, $P > 0.05$ (not significant).

revascularization or vascular maintenance by G3139-mediated, FGF2-dependent endothelial cell mitogenesis and tubular morphogenesis may produce an increase in oxygen and nutrient delivery to local cancer cells. This, in turn, might increase local pH, diminish the number of cells in G_o, decrease hypoxia-inducible factor-1α expression and thus VEGF activity, and in general diminish vascular leakiness and promote vascular "normalization." Clinically, it is possible that this may also promote chemosensitization to DTIC, as in the GM301 trial (3). How much "revascularization" might be required? The answer is unknown, but it has been suggested that as little as 22% endothelial cell death might cause a significant decrease in microvascular density (45). The inverse may be true as well.

The stimulatory effects of G3139 on endothelial cells may also suggest a possible explanation for the relationship of overall survival to pretreatment plasma levels of LDH.[5]

What is the origin of the increased plasma levels of LDH in melanoma or in patients with any tumor? LDH is a product of anaerobic glycolysis (46), which is frequently enhanced in relatively hypoxic tumors (47). Levels of the LDH-A can be

[5] S. Agrawala et al., submitted for publication.

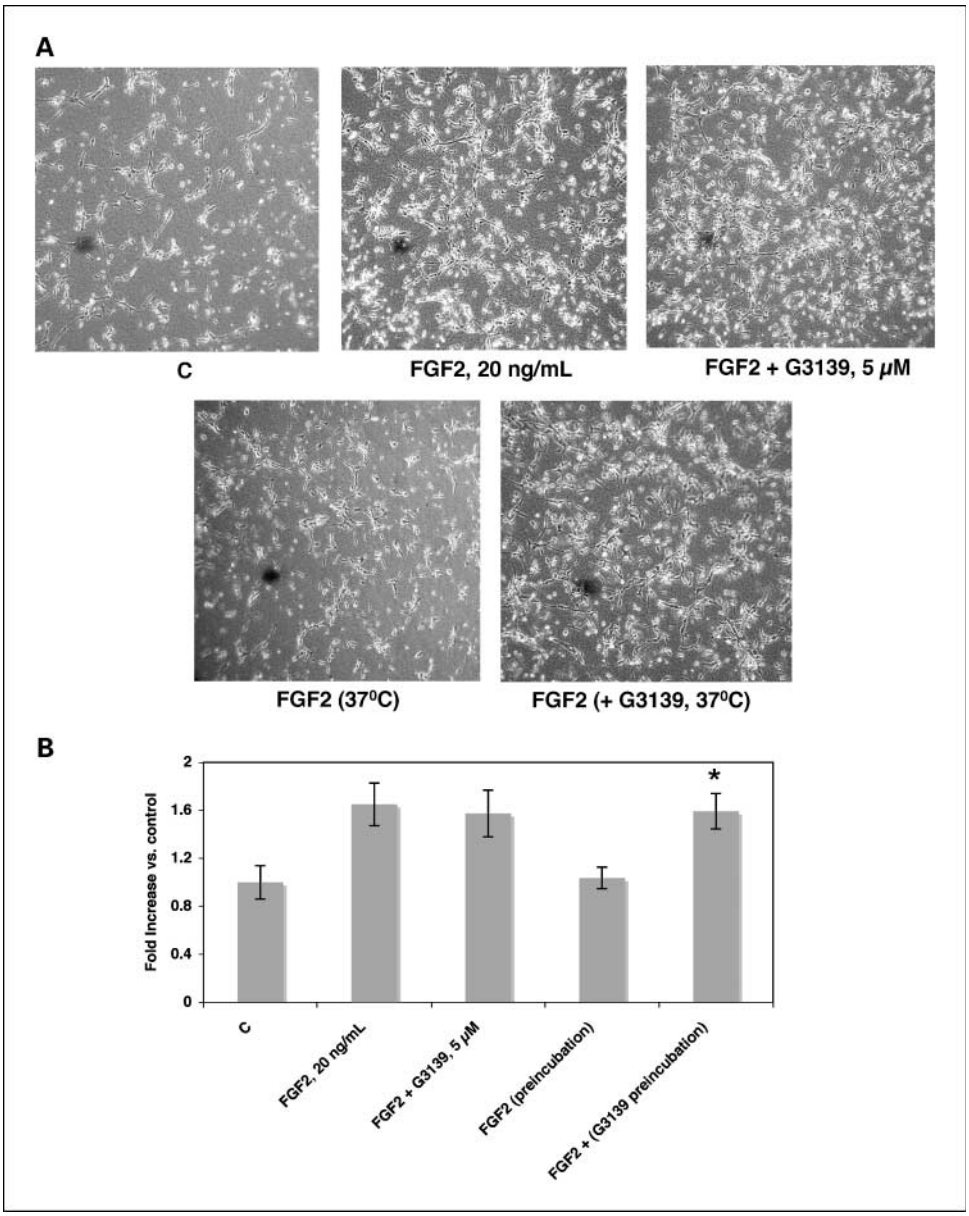

Fig. 9. G3139-protected FGF2 promotes HMEC-1 mitogenesis in three-dimensional collagen I gels. Cells (10×10^4 per well in 24-well plates) were seeded in collagen I (0.6 mg/mL) and treated with nothing (*C*), FGF2, FGF2 + G3139, or FGF2 preincubated in air (37°C, 3.5 h) with or without G3139. The cells were cultured for 7 d, photographed (*A*), and counted (*B*). Columns, average of triplicate wells; bars, SD. *, $P < 0.025$, FGF2 + G3139 in preincubation mix versus FGF2 without G3139 in preincubation mix.

up-regulated due to activation of its upstream transcription factor, the hypoxia sensor hypoxia-inducible factor 1α(48). LDH is a long-recognized, standard marker of cellular necrosis, in which, unlike in apoptosis, the cell membrane ruptures and intracellular contents spill into the surrounding space. Cells tend to undergo necrosis when they can no longer produce sufficient ATP to cover their metabolic requirements (49). This can occur in the setting of profound hypoxia, suggesting that tumor cell necrosis, as well as LDH spillage, depends on the balance between tumor growth and the ability to supply nutrients and oxygen. In turn, this balance depends on the state of tumor vascularization. Because of the effects of G3139 on endothelial cells, we speculate that G3139 may affect the balance between the rate of tumor growth and the rate of oxygen and nutrient delivery. This could produce complex effects on tumor biology and, hence, possibly on patient prognosis. However, confirmation of this speculation requires extensive *in vivo* measurements of intratumoral angiogenesis, blood flow, and tumor hypoxia, which are beyond the scope of the current study.

Disclosure of Potential Conflicts of Interest

C.A. Stein, oligonucleotide patent holder, royalty recipient, NIH; unpaid consultant, expert testimony for EMEA, Genta.

References

1. Klasa R, Gillum A, Klem R. Oblimersen Bcl-2 antisense: facilitating apoptosis in anticancer treatment. Antisense Nucleic Acid Drug Dev 2002;12:193–212.
2. Kitada S,Takayama S, Riel K, Reed J. Reversal of chemoresistance of lymphoma cells by antisense-mediated reduction of bcl-2 gene expression. Antisense Res Dev 1994;4:71–9.
3. Bedikian A, Millward M, Pehamberger H, et al. Bcl-2 antisense (oblimersen sodium) plus dacarbazine in patients with advanced melanoma: the Oblimersen Study Group. J Clin Oncol 2006;24:4738–45.
4. Smalley K, Haass M, Brafford P, et al. Multiple

signaling pathways must be targeted to overcome drug resistance in cell lines derived from melanoma metastases. Mol Cancer Ther 2006;5:1136–44.
5. Lai J, Benimetskaya L, Khvorova A, et al. Induction of apoptosis in 518A2 melanoma cells by G3139. Mol Cancer Ther 2005;4:305–15.
6. Benimetskaya L, Lai, J, Wu S, et al. Relative Bcl-2 independence of drug induced cytotoxicity and resistance in 518A2 melanoma cells. Clin Cancer Res 2004;10:8371–9.
7. Wacheck V, Losert D, Gunsberg P, et al. Small interfering RNA targeting bcl-2 sensitizes malignant melanoma. Oligonucleotides 2003;13:393–400.
8. Gekeler V, Gimmnich P, Hofmann HP, et al. G3139 and other CpG-containing immuno-stimulatory phosphorothioate oligodeoxynucleotides are potent suppressors of the growth of human tumor xenografts in nude mice. Oligonucleotides 2006;16:83–93.
9. Ballas Z, Rasmussen W, Krieg A. Induction of natural killer activity in murine and human cells by CpG motifs in oligodeoxynucleotides and bacteria DNA. J Immunol 1996;157:1840–5.
10. Lopes de Menezes A, Hudon N, McIntosh N, et al. Molecular and pharmacokinetic properties associated with the therapeutics of bcl-2 antisense oligonucleotide G3139 combined with free and liposomal doxorubicin. Clin Cancer Res 2000;6:2891–902.
11. Santel A, Aleku M, Keil O, et al. A novel si-RNA-lipoplex technology for RNA interference in the mouse vascular endothelium. Gene Ther 2006;13:1222–34.
12. Guvakova M, Yakubov L, Vlodavsky I, et al. Phosphorothioate oligodeoxynucleotides bind to basic fibroblast growth actor, inhibit its binding to cell surface receptors, and remove it from low affinity binding sites on extracellular matrix. J Biol Chem 1995;270:2620–7.
13. Yakubov L, Khaled Z, Zhang L-M, et al. Oligodeoxynucleotides interact with recombinant CD4 at multiple sites. J Biol Chem 1993;268:18818–23.
14. Cheng Y, Prusoff W. Relationship between the inhibition constant and the concentration of inhibitor which causes 50% inhibition (I50) of an enzymatic reaction. Biochem Pharmacol 1973;22:3099–108.
15. Ishai-Michaeli R, Svahn C, Weber M, et al. Importance of size and sulfation of heparin in release of basic fibroblast growth factor from the vascular endothelium and extracelllar matrix. Biochemistry 1992;31:2080–8.
16. Vernon RB, Sage EH. A novel, quantitative model for study of endothelial cell migration and sprout formation within three-dimensional collagen matrices. Microvasc Res 1999;5:118–33.
17. Nicosia R, Zhu W-H. Rat aortic ring assay of angiogenesis. Methods Endothelial Cell Biol 2004;13:125–43.
18. Benimetskaya L, Wu S, Voskresenskiy A, et al. Angiogenesis-alteration by defibrotide: implications for its mechanism of action in severe hepatic veno-occlusive disease. Blood 2008;112:4343–52.
19. Rapraeger A, Guimond S, Krufka A, Olwin B. Regulation by heparan sulfate in fibroblast growth factor signaling. Methods Enzymol 1994;245:219–40.
20. Folkman J, Klagsbrun M, Sasse J, et al. A heparin-binding angiogenic protein—basic fibroblast growth factor—is stored within basement membrane. Am J Pathol 1988;130:393–400.
21. Baird A, Ling N. Fibroblast growth factors are present in the extracellular matrix produced by endothelial cells *in vitro*: implications for a role of heparinase-like enzymes in the neovascular response. Biochem Biophys Res Commun 1987;142:428–35.
22. Powers C, McLeskey S, Wellstein A. Fibroblast growth factors, their receptors and signaling. Endocr Relat Cancer 2000;7:165–97.
23. Ornitz D, Yayon A, Flanagan J, et al. Heparin is required for cell-free binding of basic fibroblast growth factor to a soluble receptor and for mitogenesis in whole cells. Mol Cell Biol 1992;12:240–7.
24. Yayon A, Klagsbrun M, Esko J, et al. Cell surface, heparin-like molecules are required for binding of basic fibroblast growth factor to its high affinity receptor. Cell 1991;64:841–8.
25. Volkin D, Tsai P, Dabora, J, et al. Physical stabilization of acidic fibroblast growth factor by polyanions. Arch Biochem Biophys 1993;300:30–41.
26. Liu Y, Senger D. Matrix-specific activation of Src and Rho initiates capillary morphogenesis of endothelial cells. FASEB J 2004;18:457–68.
27. Whelan M, Senger D. Collagen I initiates endothelial cell morphogenesis by inducing actin polymerization through suppression of cyclic AMP and protein kinase A. J Biol Chem 2003;278:327–34.
28. Flaumenhaft R, Moscatelli D, Rifkin D. Heparin and heparan sulfate increase the radius of diffusion and action of basic fibroblast growth factor. J Cell Biol 1990;111:1651–5.
29. Akimoto T, Hammerman M. Fibroblast growth factor 2 promotes microvessel formation from mouse embryonic aorta. Am J Physiol Cell Physiol 2003;284:C371–7.
30. Alavi A, Acevedo L, Min W, Cheresh D. Chemoresistance of endothelial cells induced by basic fibroblast growth factor depends on raf-1-mediated inhibition of the proapoptotic kinase, ASK1. Cancer Res 2007;67:2766–72.
31. Seghezzi G, Patel S, Ren C, et al. Fibroblast growth factor-2 (FGF-2) induces vascular endothelial growth factor (VEGF) expression in the endothelial cells of forming capillaries: an autocrine mechanism contributing to angiogenesis. J Cell Biol 1998;141:1659–73.
32. Claffey K, Abrams K, Shih S-C, et al. Fibroblast growth factor 2 activation of stromal cell vascular endothelial growth factor expression and angiogenesis. Lab Invest 2001;81:61–75.
33. Presta M, Dell-Era P, Mitola S. Fibroblast growth factor/fibroblast growth factor receptor system in angiogenesis. Cytokine Growth Factor Rev 2005;16:159–78.
34. Jih Y, Lien W, Tsai W, et al. Distinct regulation of genes by FGF2 and VEGF-A in endothelial cells. Angiogenesis 2001;4:313–21.
35. Ribatti D, Nico B, Morbidelli L, et al. Cell-mediated delivery of fibroblast growth factor-2 and vascular endothelial growth factor onto the chick chorioallantoic membrane: endothelial fenestration and angiogenesis. J Vasc Res 2001;38:389–97.
36. Richardson P, Murakami C, Jin Z, et al. Multi-institutional use of Defibrotide in 88 patients after stem cell transplant with severe veno-occlusive disease and multi-system organ failure: response without significant toxicity in a high-risk population and factors predictive of outcome. Blood 2002;100:4337–43.
37. Jain R. Normalization of tumor vasculature: an emerging concept in anti-angiogenic therapy. Science 2005;307:58–62.
38. Jain R. Normalizing tumor vasculature with anti-angiogenic therapy: a new paradism for combination therapy. Nat Med 2001;7:987–9.
39. Semenza G. Targeting HIF-1 for cancer therapy. Nat Rev Cancer 2003;3:721–32.
40. Iervolino A, Trisciuolgio D, Ribatti D. Bcl-2 overexpression in human melanoma cells increases angiogenesis through VEGF mRNA stabilization and HIF-1 mediated transcriptional activity. FASEB J 2002;16:1453–5.
41. Cairns R, Kalliomaki K, Hill R. Acute (cyclic) hypoxia enhances spontaneous metastasis of KHT murine tumors. Cancer Res 2001;61:8903–8.
42. Rofstad E, Rasmusse, H, Galappathi K, et al. Hypoxia promotes lymph node metastasis in human melanoma xenografts by up-regulating the urokinase type plasminogen activator receptor. Cancer Res 2002;62:1847–53.
43. Pennacchietti S, Michieli P, Galluzzo M, et al. Hypoxia promotes invasive growth by transcriptional activation of the met proto-oncogene. Cancer Cell 2003;3:347–61.
44. Vaupel P. Tumor microenvironmental physiology and its implications for radiation oncology. Semin Radiat Oncol 2004;14:198–206.
45. Dong Z, Zeitlin D, Song W, et al. Level of endothelial cell apoptosis required for a significant decrease in microvessel density. Exp Cell Res 2007;313:3645–57.
46. Fantin V, St.-Pierre J, Leder P. Attenuation of LDH-A expression uncovers a link between glycolysis, mitochondrial physiology and tumor maintenance. Cancer Cell 2006;9:425–34.
47. Corn P, Ricci M, Scata K, et al. Mxi1 is induced by hypoxia in a HIF-1 dependent manner and protects cells from c-myc-induced apoptosis. Cancer Biol Ther 2005;4:1285–94.
48. Ebert B, Bunn H. Regulation of transcription by hypoxia requires a multiprotein complex that includes hypoxia-inducible factor 1, an adjacent transcription factor and p300/CREB binding protein. Mol Cell Biol 1998;18:4089–96.
49. Nasu R, Kimura H, Akagi T, et al. Blood flow influences vascular growth during tumor angiogenesis. Br J Cancer 1999;79:780–6.